

Determination of a crack's size on the basis of the non-destructive testing with eddy currents using metaheuristics

Abstract. This paper introduces a procedure for finding the position, length, depth, and width of a crack within a material, based on eddy current non-destructive testing. The measured values of the magnetic flux density are used for the crack parameters' identification. The crack's position and length are found by considering the differences in the measured magnetic flux densities between neighbouring measurement points. The crack's depth and width are found by using a stochastic optimization method connected with a finite element model.

Streszczenie. W niniejszym artykule przedstawiono procedurę znajdowania położenia, długości, głębokości i szerokości pęknięć w materiale, w oparciu o badania nieniszczące z zastosowaniem prądów wirowych. Zmierzone wartości gęstości strumienia magnetycznego są wykorzystywane do identyfikacji parametrów pęknięć. Położenie i długość pęknięcia określa się poprzez różnice w zmierzonych gęstościach strumienia magnetycznego między sąsiednimi punktami pomiarowymi. Głębokość i szerokość pęknięcia można znaleźć za pomocą stochastycznej metody optymalizacji powiązanej z modelem elementów skończonych. (Określenie wielkości pęknięcia na podstawie nieniszczących badań z zastosowaniem prądów wirowych za pomocą metaheurystyki)

Keywords: finite element method, heuristic method, non-destructive testing, magnetic field.

Słowa kluczowe: metoda elementów skończonych, metoda heurystyczna, badania nieniszczące, pole magnetyczne

Introduction

Non-destructive testing is now used more and more often for the testing of materials [1-4]. One of non-destructive methods is testing using eddy currents. In this testing case we measure the magnetic flux density within the vicinity of the tested material which has changed because of the material damage [5-9].

Our problem is a conductive plate with a crack, and is limited to a crack of rectangular geometry having a constant depth. The crack's position, crack's length l , crack's depth d and crack's width w must be found.

The first part of the research was searching for the crack's position and length. These were found by consideration of the differences between the measured magnetic flux densities and the neighbouring measurement points.

Second, the more complex part of the research was searching for the crack's depth and width. We used differential evolution [10-13] for determining the crack's depth and width. The Finite Element Method (FEM) [1, 3] model was used for the evaluation of cost function.

Measurements

Measurements were carried out for two test-cases. These were two plates, the first made of aluminium and the second of austenitic stainless steel, both of 30 mm thickness and dimensions of 330 x 285 mm. The cracks of both plates were the same and had lengths of 40 mm, depths of 10 mm, and widths of 0.5 mm. The cracks were in the middle of their respective plates.

The used measuring system, together with the test plate, is shown in Fig. 1.

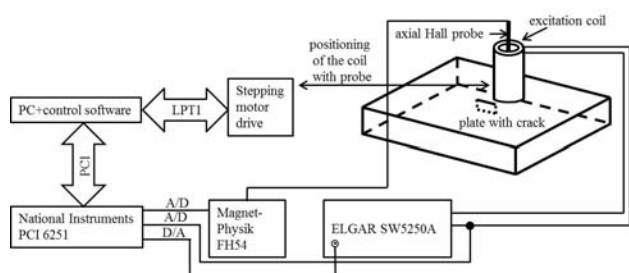


Fig.1. Measuring system

The excitation coil had an inner diameter of 36.8 mm, an outer diameter of 53 mm, and a height of 56 mm. It had 566 turns and was supplied with a sinusoidal current of 1A and a frequency of 500 Hz. An axial Hall-probe HS-AGB5-4805 was placed within a bore at the centre of the coil. The Hall probe measured the z component of the magnetic flux density. When, in the continuation of the paper, we talk about the magnetic flux density above the plate, we mean the z component of the magnetic flux density.

The position of the coil, together with the Hall-probe, was changed by the use of a stepping-motor. The step in the x direction was approximately 0.2 mm and in the y direction approximately 0.4 mm. The result of the measurement was the measured value of the magnetic flux density z-component in each position of the measuring coil. The result can be presented by the surface over the plate. Because eddy currents were absent in the area of the crack, the magnetic flux density above the crack was higher than the magnetic flux density above the plate without the crack.

The control software was developed with the use of Lab-View. The control software positioned the coil together with the Hall-sensor and captured the measured values. Figure 2 shows the results of the measurements above the aluminium plate.

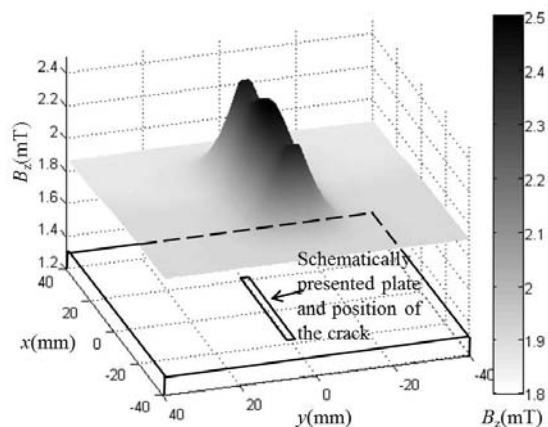


Fig.2. Measuring results above the aluminium plate

Determination of crack's position and crack's length

The position and crack's length were determined by considering the changes between the measured magnetic flux densities - calculated based on the derivatives on the surface in measured points.

The derivatives calculated from the centre point towards eight neighbouring points were calculated analytically and expressed using angles. The obtained angle can be positive if the magnetic flux density in the neighbouring point is higher, negative if in the neighbouring point it is lower or approximately zero if in the neighbouring point it is approximately the same as the magnetic flux density at the centre point. We can define the crack position and length if we know the maximum and minimum angles, which are found between the eight angles calculated for each measuring point.

The crack occurs depending on the values of the minimum and maximum angles, as presented in Table 1.

Table 1. Crack depending on the minimum and maximum angles

Minimum angle	Maximum angle	Crack
≈ 0	≈ 0	NO
≈ 0	> 0	NO
< 0	> 0	NO
< 0	≈ 0	YES
< 0	< 0	YES

The results for the test example of the aluminium plate are presented in Fig. 3.

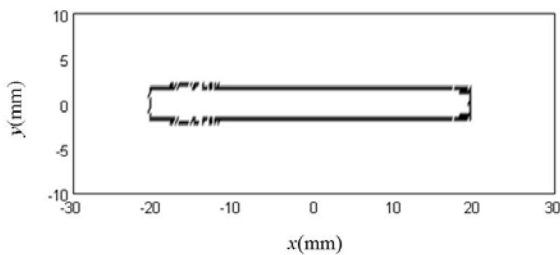


Fig.3. Position and length of the crack

From Fig. 3 we can determine the length of the crack, which was 39.4 mm. We obtained the same result in the case of the austenitic stainless steel plate.

Determination of crack's depth and crack's width

Our goal was also to determine the crack's depth and width. We did not know the values of the crack's depth and width, but we did know the magnetic flux density for each measured point above the plate. If we want to calculate the magnetic flux density for a certain point, we must create a model. As already explained, we used a differential evolution for determining the crack's depth and width.

Each magnetic flux density was measured from different coil positions. This means that new FEM calculations must be done when calculating the magnetic flux densities at each point. It is because of this that we selected only certain points as the bases for the depth and width determinations. We thus chose those points which were along a line perpendicular to the crack, as presented schematically in Fig. 4.

The measured values at the selected points, as presented in Fig. 4, depend on the crack's depth and width. Using the FEM model we searched for such values of depth and width where the calculated values at these points were as close as possible to the measured values.

The finite element mesh was made in such a way that the bands of the finite elements were parallel with the crack, so we could only adjust the crack's width by moving the finite element mesh nodes. The used finite elements were prisms with the basic plane lying within the xy plane. We

could change the crack's depth by changing the finite element's height.

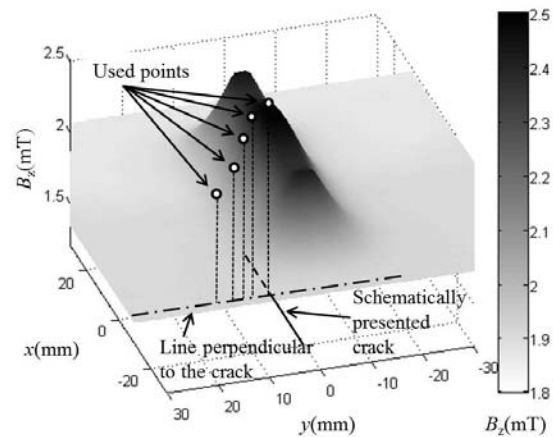


Fig.4. Points used for the depth and width determination

Using our own FEM software connected with differential evolution allowed us to make a calculation of d and w within a continuous process. The calculation procedure, together with the differential evolution, is presented in Fig. 5.

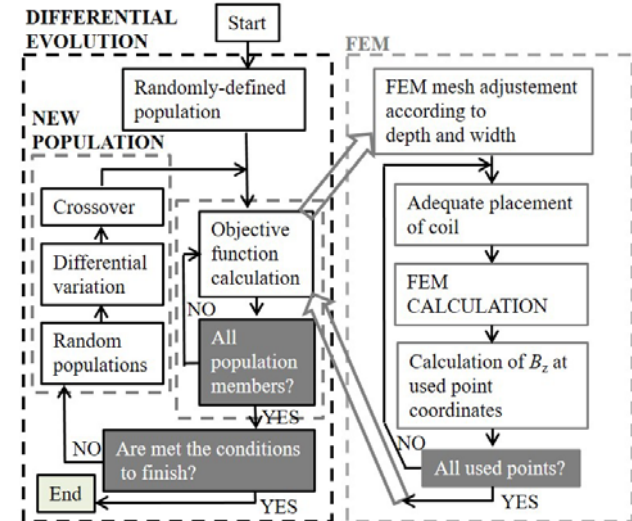


Fig.5. Flow chart of the calculation procedure

The objective function (cost function) was calculated for each pair (depth and width) of the population. We defined the objective function as the sum of the squares of the differences in the measured and calculated magnetic flux densities, expressed using (1).

$$(1) \quad f = \sum_{i=1}^n (B_{i_calculated} - B_{i_measured})^2$$

n being the number of the points used, presented in Fig. 4. The calculation procedure was finished if the predicted value of the objective function was reached or if the best pair for depth and width after the higher number of iterations did not change any more or simply after a greater number of iterations.

Calculating examples

We solved the problem using two parameters, which are the crack's depth and width. Crossover probability was set to 0.8 and Amplification of the differential variation was set to 0.6. Differential evolution strategy was DE/rand/1/bin.

The lower border of the crack's depth was set to 5 mm and the upper border to 15 mm. The lower border of the

crack's width was set to 0.2 mm and the upper border to 1 mm. Calculations were made for number of the population's members (*NPMs*), which was 10.

Aluminium plate

Two calculation iterations and results for the aluminium plate are presented in Fig. 6. Because of the stochastic features of the differential evolution, the calculation

procedure was different each time. Both the presented calculation procedures led us to the similar results. Calculation was made until the objective function was smaller than $1.5 \cdot 10^{-10}$. For the aluminium plate we know, on the basis of the investigations, that the results would be obtained if the objective function were smaller than the given value.

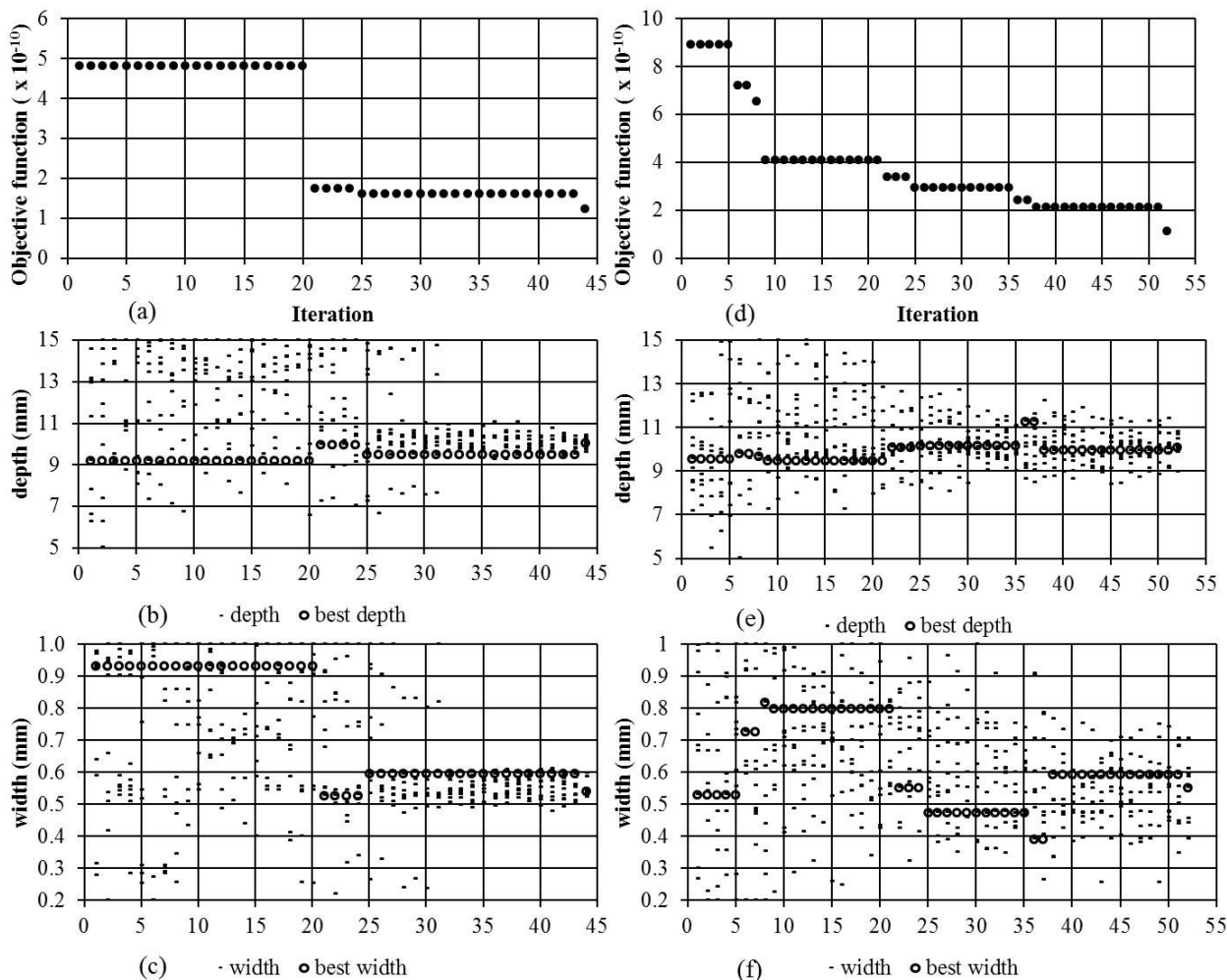


Fig.6. Aluminium plate with set *NPM* equals 10 (a) 1st calculation objective function, (b) 1st calculation depth, (c) 1st calculation width, (d) 2nd calculation objective function, (e) 2nd calculation depth, (f) 2nd calculation width.

Four points were the basis for the depth and width calculations. These points are shown in Table 2.

Table 2. Four measured points used for the calculation

Point	<i>y</i> (mm)	<i>B</i> _{measured} (mT)
1	0	2.489
2	1.693	2.481
3	2.117	2.462
4	4.657	2.29

Table 3. Calculated results for aluminium plate

Calculation	1	1
Depth (mm)	10.04796	10.08355
Width (mm)	0.54016	0.55238
Objective function	$1.215 \cdot 10^{-10}$	$1.114 \cdot 10^{-10}$
Deviation of <i>d</i> (%)	0.48	0.84
Deviation of <i>w</i> (%)	8.03	10.48

Points were selected along the line perpendicular to the crack on the *y*(mm) positions from the centre of the crack, as it is shown schematically in Fig. 4.

The calculation results are presented in Table 3.

The deviation of the calculated *d* was small, but the deviation of the calculated *w* was around 10%. The calculated *w* was not so exact because the problem was poorly conditioned in the sense of the crack's width. Figure 7 shows the objective function in the case of the aluminium plate in order to show the complexities of solving a considered inverse problem.

The objective function, as is defined by (1), was calculated for *d* at between 5 and 15 mm with a step of 0.5 mm and for *w* between 0.2 and 1 mm with a step of 0.05 mm. The above upper and lower values of *d* and *w* were also the limits of the parameters in the differential evolution. A differential evolution can set any combination of *d* and *w* within the range of the given boundaries, while the figure shows only some values of the objective function calculated for the mentioned combinations of *d* and *w*. Objective functions were not smooth as a result of the comparison between measured and calculated values. The accuracy of the measuring system and also errors and discrepancies can appear during the measuring process. The calculated values were obtained using the FEM model which is made

of 92444 3D finite elements and 50748 nodes. Also, in this case, certain numerical errors and deviations may occur. Fig. 7(b) is a part of Fig. 7(a) in order to obtain a better picture of the objective function within the area of the actual d and w .

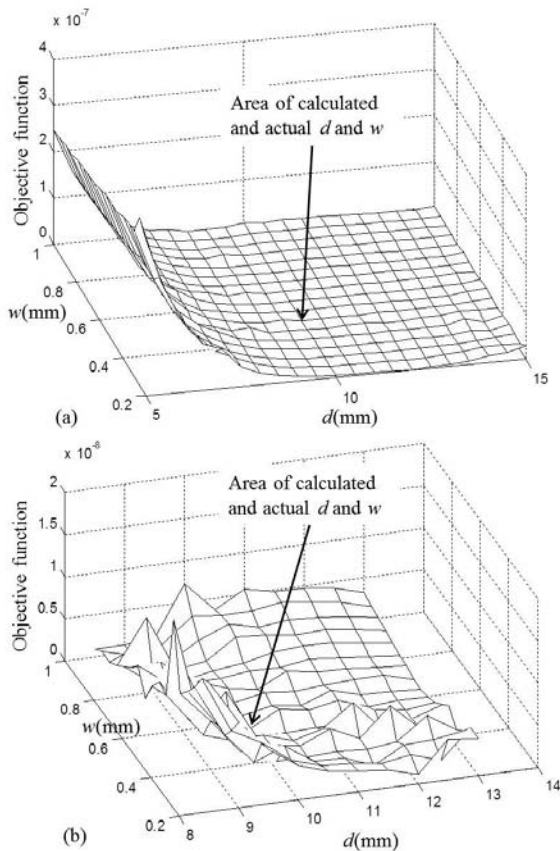


Fig.7. (a) Objective function for d between 5 and 15 mm and w between 0.2 and 1 mm, (b) Objective function for d between 9 and 13 mm and w between 0.2 and 1 mm.

Austenitic stainless steel plate

We did not know the value of the objective function which must be reached for the austenitic stainless-steel plate. It was because of this that we decided to finish the calculation after 100 iterations. Five points were the bases for the depth and width calculations. These points are shown in Table 4.

Table 4. Five measured points used for the calculation

Point	y (mm)	B_{measured} (mT)
1	1.693	5.1384
2	2.117	5.1384
3	5.503	5.1244
4	8.043	5.1244
5	16.933	5.0974

Table 5. Calculated results for austenitic stainless steel plate

Calculation	1	2
Depth (mm)	10.96073	11.05926
Width (mm)	0.54612	0.55877
Objective function	$3.615 \cdot 10^{-11}$	$4.367 \cdot 10^{-11}$
Deviation of d (%)	9.61	10.59
Deviation of w (%)	9.22	11.75

The points were selected along the line perpendicular to the crack at the y (mm) positions from the centre of the crack, as is shown schematically in Fig. 4. The calculated results are presented in Table 5.

Based on the observation of the calculation procedure, we found that 100 iterations was sufficient. The best pair had not changed for a larger number of iterations. We can

see from Table 5 that the deviation of d and w was around 10%. The results were not as good as in the case of the aluminium plate. The reason was in the sensitivity of the measuring system. The conductivity of the austenitic stainless-steel plate was lower than the conductivity of the aluminium plate. Consequently, the difference between the measured magnetic flux density within the area of the crack and within the area without the crack was much lower. The sensitivity of the measurement system was the same for both test cases, which means that the measurements in the case of aluminium plate were more accurate.

Conclusions

A differential evolution is appropriate for the described problem because it is able to overcome any local minimums which might appear because of measurement or calculation inaccuracies. Despite the very sensitive problem, and the measuring and FEM calculation mistakes, the differential evolution was stable and gave us correct results for all six test calculations.

Authors: Assistant professor Marko Jesenik, University of Maribor, Faculty of Electrical Engineering and Computer Science, Koroška cesta 46, 2000 Maribor, Slovenia, E-mail: marko.jesenik@um.si; Full professor Anton Hamler, University of Maribor, Faculty of Electrical Engineering and Computer Science, Koroška cesta 46, 2000 Maribor, Slovenia, E-mail: anton.hamler@um.si; Assistant professor Miloš Beković, University of Maribor, Faculty of Electrical Engineering and Computer Science, Koroška cesta 46, 2000 Maribor, Slovenia, E-mail: milos.bekovic@um.si; Full professor Mladen Trlep, University of Maribor, Faculty of Electrical Engineering and Computer Science, Koroška cesta 46, 2000 Maribor, Slovenia, E-mail: mladen.trlep@um.si

REFERENCES

- [1] Zeng Z., Udpa L., Udpa S.S., Finite-element model for simulation of ferrite-core eddy-current probe, *IEEE Trans. on Magn.*, 46 (2010), 905-909
- [2] Zeng Z., Udpa L., Udpa S.S., Chan M.S.C., Reduced magnetic vector potential formulation in the finite element analysis of eddy current non-destructive testing, *IEEE Trans. on Magn.*, 45 (2009), 964-967
- [3] Vasić D., Bilas V., Šnajder B., Analytical modelling in low-frequency electromagnetic measurements of steel casing properties, *NDT&E Int.*, 40 (2007), 103-111.
- [4] Yuso N., Perrin S., Mizuno K., Miya K., Numerical modelling of general cracks from the viewpoint of eddy current simulations, *NDT&E Int.*, 40 (2007), 577-583
- [5] Theodoulidis T., Poulakis N., Ventre S., Rapid computation of eddy current signals from narrow cracks, *NDT&E Int.*, 43 (2010), 13-19
- [6] Rubinacci G., Tamburrino A., Ventre S., An efficient numerical model for a magnetic core eddy current probe, *IEEE Trans. on Magn.*, 44 (2008), 1306-1309
- [7] Pascaud C.G., Pietantoni M., Eddy current array probe development for non-destructive testing, *16th World Conference on NDT (Montreal, Canada)*, (2004)
- [8] Fan M., Huang P., Ye B., Hou D., Zhang G., Zhou Z., Analytical modelling for transient response in pulse eddy current testing, *NDT&E Int.*, 41 (2009), 376-383
- [9] Zaoui A., Menana H., Feliachi M., Berthiau G., Inverse problem in nondestructive testing using arrayed eddy current sensors, *OPEN ACCESS sensors*, 10 (2010), 8696-8704
- [10] Haupt R.L., Haupt S.E., *Practical Genetic Algorithms, second edition*, A John Wiley & Sons, inc. publication, (2004)
- [11] Qing A., Lee C.K., *Differential Evolution in Electromagnetics*, Springer-Verlag Berlin Heidelberg, (2010), 19-42
- [12] Qing A., Dynamic differential evolution strategy and applications in electromagnetics inverse scattering problems, *IEEE Trans. on Magn.*, 44 (2006), 116-125
- [13] Rocca P., Oliveri G., Massa A., Differential Evolution as Applied to Electromagnetics, *IEEE Antennas and Propagation Magazine*, 50 (2011), 38-49